Diode laser forming of stainless steel tubes

A. Guglielmotti[1], F. Quadrini[1], E.A. Squeo[1], V. Tagliaferri[1]

[1]*University of Rome "Tor Vergata", Department of Mechanical Engineering*
Via del Politecnico 1, 00133 Rome, Italy
URL: www.mec.uniroma2.it *e-mail: guglielmotti@ing.uniroma2.it;*
quadrini@ing.uniroma2.it;
squeo@ing.uniroma2.it;
tagliaferri@ing.uniroma2.it

L'ABSTRACT: In this study, complex tube bending operations were carried out by means of laser forming. Bending of slotted tubes was discussed as well as enlarging of one tube end. Experimental tests were performed on AISI 304 stainless steel tubes with a thickness of 1 mm and an outer diameter of 20 mm. A high power diode laser (HPDL) was used in focalization condition. In order to design the new processes, a finite element (FE) model was developed, which allowed the tube deformation under laser processing. The numerical model was experimentally validated and was used to study the physical phenomena occurring during the forming process. The thermo-mechanical problem was decoupled and solved sequentially in two phases: a transient thermal analysis to obtain temperature distribution that was input as body load for the following static analysis. HPDLs are very efficient laser sources for tube forming due to their large laser spot.

Key words: Tube bending, Diode laser, Stainless steel, Numerical modelling

1 INTRODUCTION

Laser forming is a no-contact technique for sheet metal and tube forming: the bending is obtained because of the difference between the very fast heating rate (under laser exposure) and the subsequent slow cooling rate after the laser removal. In the last 15 years laser forming was investigated more and more due to the interesting applications in manufacturing industries. Laser sources have many advantages in terms of compactness, energy efficiency, lifetime and running cost. In 2000, Li discussed the application of high-power diode laser in material processing such as soldering, surface treatment, welding, marking, sheet metal bending [1]. Among these applications, laser forming is a valid technique due to the high degree of control over the energy transfer, the high accuracy and reliability, the very high flexibility and the non-contact nature of the process [2]. In particular, laser bending of thin sheets is achieved by plastic deformation induced by thermal stresses, which results from rapid material heating and cooling. Due to the no-contact nature of the process, hard tooling is not necessary and small batch production runs and rapid prototyping are very effective applications.

Several scientific studies deal with laser bending of tubes and the related physical mechanisms. Li and Yao discussed in detail the mechanism at the basis of laser tube bending by stress analysis [3]. Subsequently, Hao and Li, performed a thermo-mechanical simulation to correlate stress rising in the tube and thermal gradients [4]. Safdar et al. discussed the main parameters to control the bending process and the correlation between thermal stresses, laser beam geometry and scanning direction [5].

The current study deals with an innovation in laser tube bending in terms of complexity of the shaped tubes. Slotted tubes were considered as well as circumferential scanning paths. A numerical model was also defined to study the physical mechanisms at the basis of the proposed results and to design innovative applications.

A stainless steel tube with a thin cross section was used for the experimentation and the laser power was kept at 150 W.

2 NUMERICAL MODELLING

A finite element model (FEM) was defined to investigate the tube forming under different process conditions. The model was built in ANSYS 9 by means of the parametric design language (APDL) to reduce modelling and solution times.
In order to calibrate the numerical procedure, only one tube configuration was taken into account, whereas in the following experimental section three different configurations are discussed. In particular, an AISI 304 tube with a complex slot was modelled (figure 1). The tube was 50 mm in length, 20 mm in outer diameter and 1 mm in wall thickness. The U-shaped slot was 15 mm long and 10 mm wide. The tube geometry was divided into 3 parts for discretising. The internal part, where the spot acted, was mapped meshed with a fine mesh. Also the two external parts were mapped meshed but with a coarse mesh. The number of element divisions along the tube thickness was 3 in each part of the tube. The laser heating was modelled by means of a thermal load in terms of heat flux over a 3.8x1.2 mm^2 rectangular spot as figure 1 shows. A 150 W power was considered for the laser beam. After the calibration procedure, the absorption coefficient was set to 0.5 and the heat transfer coefficient was 21 $W/(m^2K)$. The tube rotation was modelled by performing a spot revolution along the portion of the external circumference delimitated by the slot boundaries (about 56°). At each time step, the spot moved so as to overlaps for a half to the previous position. Fixing the rotational speed to 0.628 rad/s, the resulting time step depended only on the mesh size and was nearly 0.085 s.

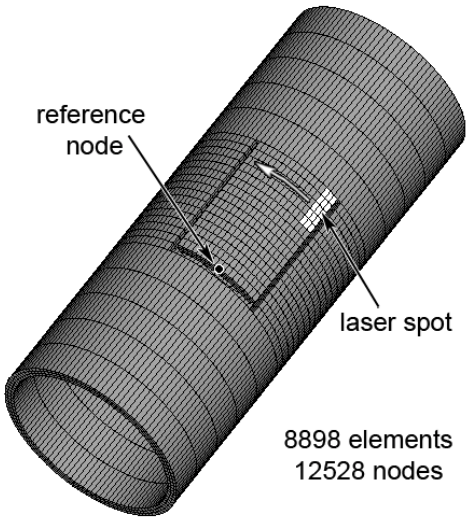

Fig. 1. FEM model for laser forming

After each laser heating step, a cooling step of 80 s was simulated. Ten heating-cooling cycles were performed. The material properties were implemented as a function of temperature, according to [6]. A thermo-mechanical analysis was performed to simulate the forming process. Thermal analysis was carried out by using SOLID70 thermal elements. After obtaining the thermal solution, the thermal elements were converted into SOLID45 structural elements and the thermal solution was used to define the thermal loads. At the end of the simulation, the radial displacement of a reference node (figure 1) was evaluated.

3 MATERIALS AND METHODS

Laser forming tests were performed putting into rotation slotted tubes, made of AISI 304, under a focused HPDL beam, at a speed of 0.628 rad/s. All the tubes were 20 mm in outer diameter and 1 mm in thickness, according to the previously described FE model. In order to provide the rotational speed, the tubes were cut to a length of 50 mm and clamped to a stepping motor. The geometrical features of the tubes are depicted in figure 2. In particular, sample (a) had no slots, whereas sample (b) had a U-shaped slot and (c) had 4 symmetric slots along the tube end. The laser treated zone is shown in figure 2 with a darker colour for each sample. Sample (b) presented the same geometry discussed in the Numerical Modelling section.

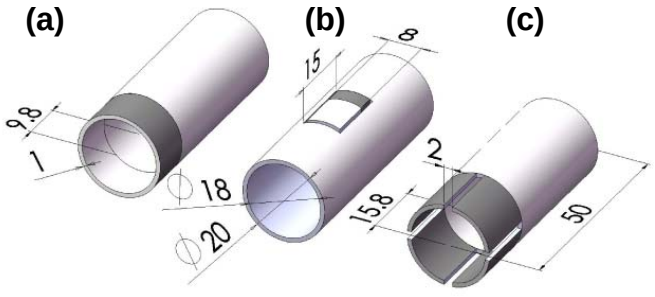

Fig. 2. Samples for laser forming tests

A 1.5 kW diode laser (Rofin-Sinar, DL 015) was used for tube forming. It had 940 nm wavelength and a rectangular spot (3.8x1.2 mm^2) due to the superposition of two different rays, each one coming from a 750 W emitter diode. A 63 mm long focus lens was used to maximize the depth of field. During tests, the laser beam was focused on the external tube surface and the laser power was fixed at 150 W. The tube clamping length was 15 mm. The details

about the scanning schemes are reported in Table 1. Initially the laser was focused on the tube external surface and a first scan was performed along the tube circumference. At the end of the scan the laser spot was moved to the initial position to repeat the same scan. Up to a maximum of 20 scans were performed consecutively. At the end of this first set of scans, the tube was left to cool in air. Subsequently the laser spot was moved along the tube length to perform a set of scans on a parallel circumferential line. Finally, the total processed length of the tube ranged from 9.8 to 15.8 mm, the number of scans per circumferential line from 10 to 20. The single laser scan interested the entire tube external circumference apart from the sample (b), for which an angular dimension of 56° was considered to bend only the tongue of figure 2. The distance between two consecutive set of scans was 2 mm. As the laser spot maximum axis was aligned to the tube length, a 1.8 mm superposition resulted between successive scans.

Table1. Geometrical parameters for tube forming tests

Sample	Tube scanned length [mm]	Number of scans per line	Angular dimension of a single scan [°]	Distance between consecutive set of scans [mm]
A	9.8	20	360	2
B	3.8	10	56	0
C	15.8	20	360	2

4 RESULTS AND DISCUSSION

4.1 Numerical modelling

Figures 3 and 4 show the results of the numerical simulation in terms of radial displacement of the reference node as a function of time for 1 and 10 scans respectively. As figure 3 shows, at the beginning of the laser exposure, a sudden increase occurs due to the thermal expansion up to a maximum (point 1). In this case the laser path is too short and the constraining effect of the surrounding material determines this deformation. Subsequently, the radial displacement decreases down to a minimum (point 2). In fact after 1 s, the laser path is sufficiently longer than the spot size (figure 5). The tongue deforms entering the tube wall and the minimum displacement is negative. As the thermal strains have the same gradient of the temperature, the maximum is on the side of the spot and the tongue bends in the opposite direction. But in this condition, due to the very high temperature, the material starts to yield in the laser processed zone. When the laser spot is sufficiently far from the early processed zone, the material starts to cool. However, due to the previous yielding, the tongue cannot return in the initial configuration but it starts to bend in the opposite direction.

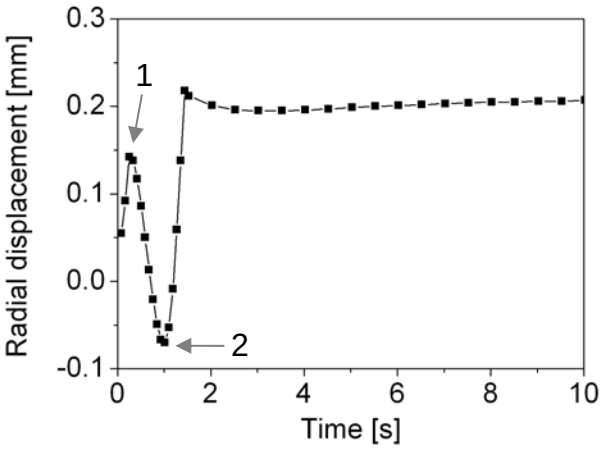

Fig. 3: Radial displacement of the reference node during the first scan

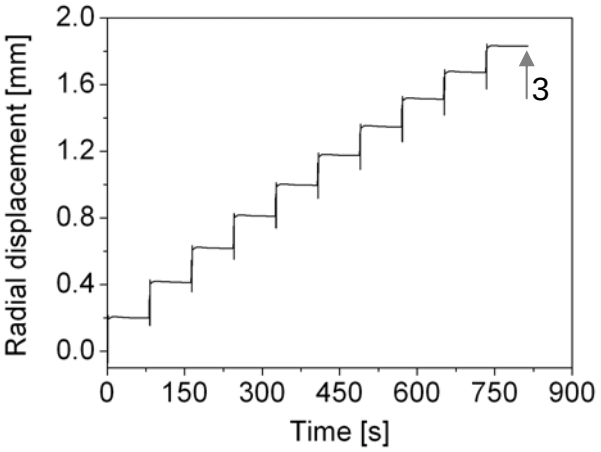

Fig. 4: Radial displacement of the reference node during 10 scans

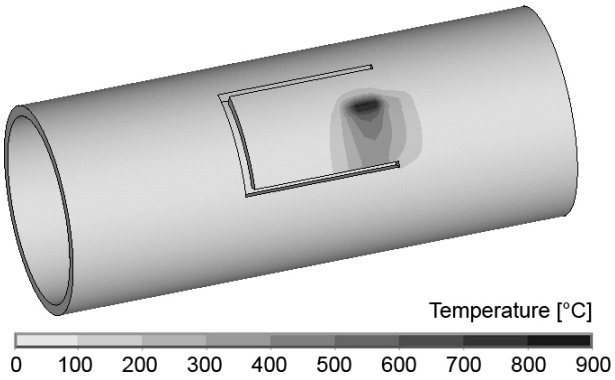

Fig. 5: Temperature map after 1 s (point 2).

figure 4 shows the effect of the successive superimposed scans. At the beginning of each step, the same mechanism of figure 3 is repeated. In particular the relative minimum is always clearly visible. After 800 s of laser processing, over 1.8 mm of total radial displacement is achieved (point 3).
In figure 6 three displacement maps are reported in correspondence of the above mentioned points. For a better understanding, maps 1 and 2 are shown with a scale factor of 10, map 3 is in true scale. It is evident the complex forming mechanism that leads the tongue to invert twice the bending direction.

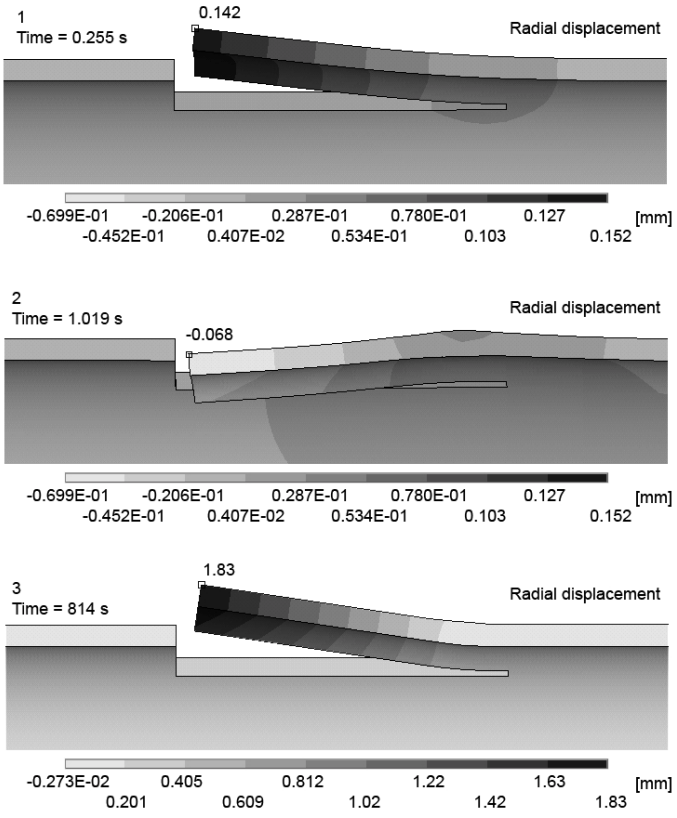

Fig. 6: Radial displacement maps (section view) at three different time steps.

The numerical simulation was validated by the experimental test on sample (b). It was measured a maximum radial displacement of about 2 mm, according to the result of figure 6.

4.2 Laser forming tests

In figure 7, the picture of the formed tubes is reported. A flare was obtained for the sample (a). In sample (b) the result was similar to the case of sheet metals and the tube wall deformed toward the laser source.
However the unprocessed surface of the tongue remained unaltered with the shape of the initial cylindrical surface. Instead, in sample (c) the laser spot was moved from one end to the other one for a distance of almost 16 mm. A complex double curvature surface resulted in the four tongues.

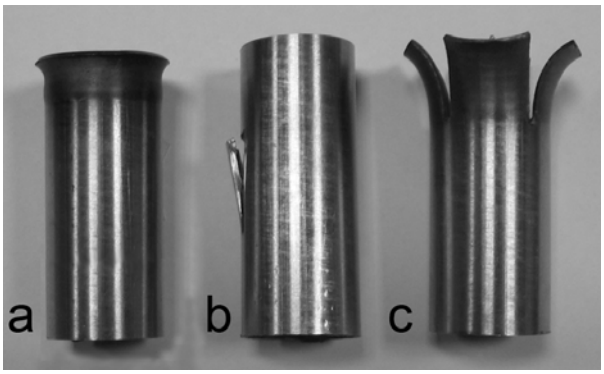

Fig. 7: Aspect of the samples after laser processing

5 CONCLUSIONS

In this study a diode laser was used to form stainless steel tubes in different conditions. Under the proposed conditions, a low power was sufficient to have a good forming efficiency considering that the tube is thin. The main topic was to allow new forming processes apart form bending. Tongues, flanges and flares can be achieved as well and used in small production runs or prototypes.

REFERENCES

1. L. Li, The advances and characteristics of high-power diode laser materials processing. *Optics and Lasers in Engineering*. 34 (2000) 231-53.
2. N. Hao and L. Li, An analytical model for laser tube bending. *Applied Surface Science*. 208-209 (2003) 432-6.
3. W. Li and Y.L. Yao, Laser Bending of Tubes: Mechanism, Analysis, and Prediction. *Journal of Manufacturing Science and Engineering*. 123 (2001) 674-81.
4. N. Hao and L. Li, Finite element analysis of laser tube bending process. *Applied Surface Science*. 208-209 (2003) 437-41.
5. S. Safdar, L. Lin, M.A. Sheikh and Z. Liu, Finite element simulation of laser tube bending: Effect of scanning schemes on bending angle, distortions and stress distribution. *Optics and Laser Technology*. 39 (2007) 1101-10.
6. J. Chen and B. Young, Stress-strain curves for stainless steel at elevated temperatures. *Engineering Structures*. 28 (2006) 229-239.